Microsyst Technol (2011) 17:997–1002
DOI 10.1007/s00542-011-1245-7

TECHNICAL PAPER

Analytical read back signal modeling in magnetic recording

Uwe Boettcher · Christopher A. Lacey · Hui Li · Kensuke Amemiya · Raymond A. de Callafon · Frank E. Talke

Received: 31 August 2010 / Accepted: 28 January 2011 / Published online: 18 February 2011

Abstract An analytical model for the read back signal is derived for perpendicular and longitudinal magnetic recording. The model captures the contribution of a single bit rather than the contribution of a bit transition which makes it applicable to patterned media as well as continuous media. It is based on the law of Biot–Savart and separates the contribution of the magnetic media from the head sensitivity function.

1 Introduction

A large number of analytical models for the magnetic read back signal have been developed in the past for longitudinal and perpendicular magnetic recording (Valcu and Bertram 2002; Roscamp et al. 2002; Smith 1993; Wood and Wilton 2008; Shute et al. 2006; Chai et al. 2006; Suzuki et al. 2006; Wilton et al. 2004; Mallinson and Bertram 1984; Radhakrishnan et al. 2007; Bertram 1994; Khizroev and Litvinov 2004; Richter 1999; Yuan and Bertram 1994, 1996; Suzuki and Nishida 2001, 2003). Initially, the "on-track" response was approximated in 2-D by neglecting off-track effects and approximating an isolated bit transition which yields a bell-shaped curve for longitudinal recording and a di-bit curve for perpendicular recording (Richter 1999). With increasing storage density and decreasing bit aspect ratio there was a need to switch from initial 2-D models to 3-D models (Wood and Wilton 2008). Many of the models developed consider isolated magnetic bit transitions (Valcu and Bertram 2002; Wood and Wilton 2008; Chai et al. 2006). A commonly used technique is based on the principle of reciprocity as applied in (Roscamp et al. 2002; Smith 1993; Chai et al. 2006; Yuan and Bertram 1994; Yuan and Bertram 1996) or Fourier components (Shute et al. 2006; Suzuki et al. 2006; Suzuki and Nishida 2001, 2003). An excellent overview of previously developed models is given in Wilton et al. (2004). In Wilton et al. (2004), the read back signal is approximated by considering various magnetic potentials.

In this paper, we are following a different approach for an analytical approximation of the read back signal which is motivated by the evolution in magnetic recording technology. Previously, inductive recording heads were used that measured the transition (derivative) of the magnetization pattern on the disk. Today, giant/ tunnel magnetoresistance (G/TMR) heads are in use that change their resistance in the presence of a magnetic field. Furthermore, one of the possible future technologies in hard disk drives might be bit patterned media (BPM) (Hughes 1999) where the magnetic bits are well separated from each other to

U. Boettcher (✉) · R. A. de Callafon · F. E. Talke
Center for Magnetic Recording Research, University of California, San Diego, 9500 Gilman Drive # 0401, La Jolla, CA 92093, USA
e-mail: uwe@ucsd.edu

R. A. de Callafon
e-mail: callafon@ucsd.edu

F. E. Talke
e-mail: ftalke@ucsd.edu

C. A. Lacey
Microphysics, Inc., 4620 Fortran Dr., Suite 120, San Jose, CA 95134, USA
e-mail: chrislacey@microphysics.com

H. Li · K. Amemiya
Storage Mechanics Laboratory, Hitachi Asia Ltd., Singapore 049318, Singapore
e-mail: hli@has.hitachi.com.sg

K. Amemiya
e-mail: kamemiya@has.hitachi.com.sg

avoid cross-talk effects at high areal densities. G/TMR and BPM will intuitively require a read back signal model that considers the measured response of the bit rather than the bit transition as the transition parameter might not be described correctly with current analytical models. Furthermore, servo designs in BPM that incorporate either only "up" or only "down" magnetized bits could be captured by the model. Track edge effects and written transitions that are sometimes modeled by an ellipse (Wood and Wilton 2008) would be decreased as the bits on patterned media would potentially have a well defined shape. More complicated shapes could be investigated by using the model developed and a so-called micro grid approach (Chai et al. 2006) that is very accurate and considerably faster than finite element solutions.

The objective of this paper is to propose a 3D analytical model of the read back signal that allows the investigation of any recorded bit pattern separated from the various different types of head sensitivity functions. This paper is organized as follows. Section 2 shows how the 3D distribution of the magnetic field can be approximated for longitudinal and perpendicular magnetic recording using the law of Biot–Savart. Thereafter, in Sect. 3, a simple model of head sensitivity is given which will be used to calculate the read back signal. Finally, in Sect. 4, the read signal for longitudinal and perpendicular recording is simulated for an example pattern.

2 Media contribution

The media magnetization is modeled considering a single point of measurement. The coordinate system is defined according to Fig. 1 which corresponds to longitudinal magnetic recording (LMR). It will be shown later that the results of the LMR system can be simply modified to perpendicular magnetic recording (PMR) through a rotation by $\frac{\pi}{2}$ and adding a soft magnetic underlayer (SUL).

For a simple analytic approach continuity of space is assumed. Therefore, it is necessary to assume that the relative permeability of the recording layer is unity for both perpendicular and longitudinal recording (Takahashi et al. 2003). As indicated in Fig. 1, each bit is assumed to have a cuboidal shape with length L, width W and recording layer thickness T. Other shapes such as cylindrical shapes could also be of interest for BPM but are beyond the scope of this paper. Each bit can be modeled as a permanent magnet which itself can be modeled by placing equivalent currents on its surface. As indicated in Fig. 1, an infinite number of equidistant currents with infinitesimal distance $d\ x$ apart from each other are placed on the bit. The origin of the coordinate system is defined in the center of the bit. Using the law of Biot–Savart (Spaldin 2003), which can be derived from Maxwell's equations, one can calculate the differential magnetic field $\mathrm{d}\mathbf{H}(\mathbf{r})$ caused by each surface current segment as

$$\mathrm{d}\mathbf{H}(\mathbf{r}) = \frac{\mathrm{I}}{4\pi}\frac{\mathbf{dl}\times(\mathbf{r}'-\mathbf{r})}{|\mathbf{r}'-\mathbf{r}|^3} \tag{1}$$

where $\mathbf{r}$ is the vector to the measurement point, $\mathbf{r}'$ is the vector to the contributing surface current segment and $\mathbf{dl}$ is the vector of the contributing surface current segment (Fig. 1). The value of each surface current equals

$$I = H_C dx \tag{2}$$

where H_C is the coercivity of the magnetic recording layer. The currents that are indicated in Fig. 1 have four main components of direction (1,2,3,4). The vector $\mathbf{r}'$ to each current segment $\mathbf{dl}$ can be parameterized for the four components of direction as

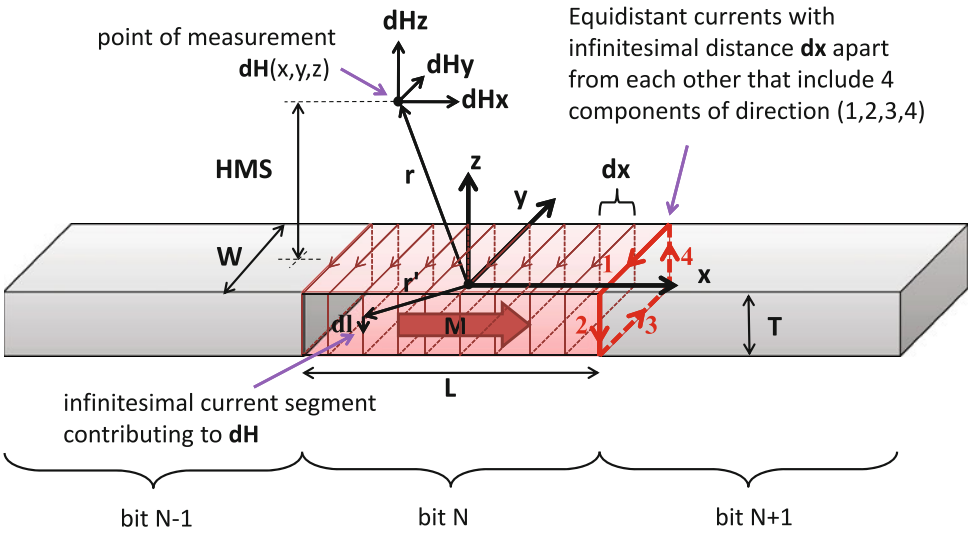

Fig. 1 Defining the coordinate system

$$\mathbf{r}_1'(x,t) = \begin{pmatrix} x \\ W/2 \\ T/2 \end{pmatrix} + t\begin{pmatrix} 0 \\ -W \\ 0 \end{pmatrix} \tag{3}$$

$$\mathbf{r}_2'(x,t) = \begin{pmatrix} x \\ -W/2 \\ T/2 \end{pmatrix} + t\begin{pmatrix} 0 \\ 0 \\ -T \end{pmatrix} \tag{4}$$

$$\mathbf{r}_3'(x,t) = \begin{pmatrix} x \\ -W/2 \\ -T/2 \end{pmatrix} + t\begin{pmatrix} 0 \\ W \\ 0 \end{pmatrix} \tag{5}$$

$$\mathbf{r}_4'(x,t) = \begin{pmatrix} x \\ W/2 \\ -T/2 \end{pmatrix} + t\begin{pmatrix} 0 \\ 0 \\ T \end{pmatrix} \tag{6}$$

Here, t ranges from 0 to 1 and x ranges from $-\frac{L}{2}$ to $\frac{L}{2}$. The vectors $\mathbf{r}_i'$ are given in (3)–(6) and each current segment $\mathbf{dl}_i$ is defined as

$$\mathbf{dl}_i = \frac{\partial \mathbf{r}_i'}{\partial t} dt \tag{7}$$

We can now compute the total magnetic field as

$$\mathbf{H}(\mathbf{r}) = \sum_{i=1}^{4} \int_{-\frac{L}{2}}^{\frac{L}{2}} \int_{0}^{1} \frac{\mathrm{H_C}}{4\pi} \frac{\frac{\partial \mathbf{r}_i'}{\partial t} \times (\mathbf{r}_i' - \mathbf{r})}{|\mathbf{r}_i' - \mathbf{r}|^3} dt\, dx \tag{8}$$

Each of the two integrals in (8) yields two components in the analytical solution of (8) and since there are four main current directions we obtain $4 \times 2 \times 2 = 16$ components for the solution of (8). We can solve this integral analytically. For clarity, we write the x-, y- and z-components of the measured magnetic field at point $\mathbf{r} = (x_m, y_m, z_m)^T$ separately in (9)–(11) as

$$H_x = \frac{\mathrm{H_C}}{4\pi} \sum_{i=1}^{16} S_i \arctan\left(\frac{\left(\frac{\mathrm{L}}{2} + \mathrm{a}_{xi} x\right) \left(\frac{\frac{\mathrm{T}}{2} + \mathrm{a}_{zi} z}{\left|\frac{\mathrm{W}}{2} + \mathrm{a}_{yi} y\right|} \right)^{\mathrm{a}_{ei}}}{R_i} \right) \tag{9}$$

$$H_y = \frac{\mathrm{H_C}}{4\pi} \sum_{i=1}^{16} \frac{\mathrm{a}_{ei}}{2} \ln\left[\mathrm{a}_{zi} \left(\mathrm{a}_{yi} \left(\frac{\mathrm{T}}{2} + \mathrm{a}_{zi} z \right) + \mathrm{a}_{xi} \mathrm{a}_{ei} R_i \right) \right] \tag{10}$$

$$H_z = \frac{\mathrm{H_C}}{4\pi} \sum_{i=1}^{16} \frac{\mathrm{a}_{ei}}{2} \ln\left[\mathrm{a}_{yi} \left(\mathrm{a}_{zi} \left(\frac{\mathrm{W}}{2} + \mathrm{a}_{yi} y \right) + \mathrm{a}_{xi} \mathrm{a}_{ei} R_i \right) \right] \tag{11}$$

where R_i and S_i are defined by

$$R_i = \sqrt{\left(\frac{\mathrm{L}}{2} + \mathrm{a}_{xi} x\right)^2 + \left(\frac{\mathrm{W}}{2} + \mathrm{a}_{yi} y\right)^2 + \left(\frac{\mathrm{T}}{2} + \mathrm{a}_{zi} z\right)^2} \tag{12}$$

and

$$S_i = \mathrm{sign}\left(\left(\frac{W}{2} + \mathrm{a}_{yi} y\right) \left(\frac{T}{2} + \mathrm{a}_{zi} z\right) \right) \tag{13}$$

respectively. The coefficients $a_{xi} \in \{-1, 1\}$, $a_{yi} \in \{-1, 1\}$, $a_{zi} \in \{-1, 1\}$ and $a_{ei} \in \{-1,1\}$ (x-, y-, z-direction and exponent) occur in all possible perturbations and are listed in Table 1. For a simple numerical example with parameters: head-medium spacing (HMS) = 10, W = 50, W = 50, T = 20 nm, the normalized media magnetization in longitudinal recording is plotted in Fig. 2. As indicated earlier, this result can be modified to obtain the solution for PMR. Figure 3a shows the cuboidal shaped bit from Fig. 1 rotated by $\frac{\pi}{2}$ around the y-axis. The contribution of the soft magnetic under layer (SUL) to the magnetic field measured at $\mathbf{r} = (x_m, y_m, z_m)^T$ has to be taken into account. The SUL has a relative permeability that is much larger than 1 (on the order of 100). For the analytical approximation it is assumed to be infinity. Therefore, an image source is placed below the bit (Fig. 3a). It can also be modeled by a mirror head (Khizroev and Litvinov 2004) as shown in Fig. 3b. Figure 3a (one head and two bits) represents the equivalent numerical problem as Fig. 3b (one bit and two heads) where the magnetic field is computed for two different points yielding the contribution of the real head H^{real} and the contribution of the image head H^{img}. An adjustment parameter $\sigma \geq 0$ is introduced that depends on the thickness and the relative permeability of the soft magnetic underlayer and the thickness of the intermediate layer. It is obvious that placing the soft magnetic layer further away from the recording layer will decrease the effect of the under layer on the read back signal. By switching x- and z-components in the coordinate system definitions (9)–(11) can be rewritten. The shielded tunnel magneto resistance (TMR) head is mainly sensitive to the z-component of the magnetic field (Wood and Wilton 2008). Hence, only the z-component is considered here. However, depending on the head design, the x- and y-components could be considered as well. H_z can be written as the superposition of the contribution of the "real" head and the "image" head as indicated in Fig. 3b. Thus, the new

Table 1 Coefficients

i	1	2	3	4	5	6	7	8
a_{xi}	1	1	1	1	1	1	1	1
a_{yi}	1	1	1	1	−1	−1	−1	−1
a_{zi}	1	1	−1	−1	1	1	−1	−1
a_{ei}	1	−1	1	−1	1	−1	1	−1
i	9	10	11	12	13	14	15	16
a_{xi}	−1	−1	−1	−1	−1	−1	−1	−1
a_{yi}	1	1	1	1	−1	−1	−1	−1
a_{zi}	1	1	−1	−1	1	1	−1	−1
a_{ei}	1	−1	1	−1	1	−1	1	−1

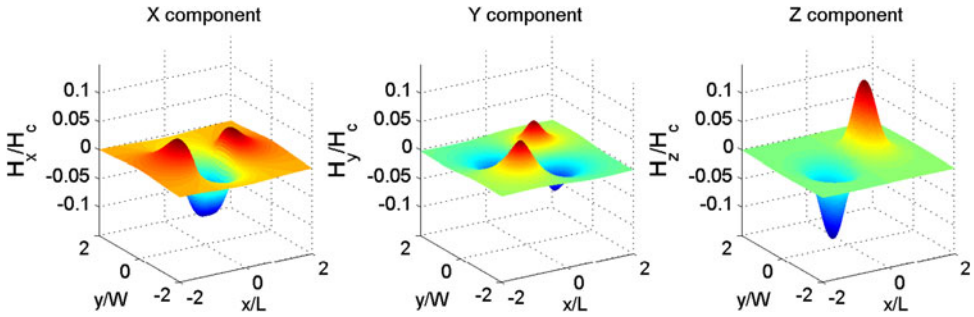

Fig. 2 Normalized magnetic field components for longitudinal magnetic recording measured at HMS = 10 for W = 50, L = 50, T = 20 nm

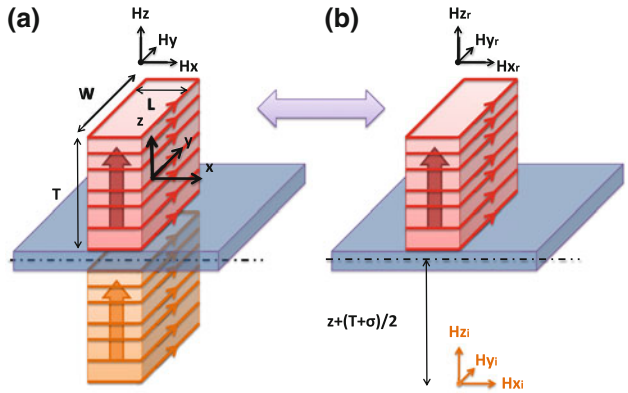

Fig. 3 Modeling perpendicular recording

z-component of the magnetic field for perpendicular recording yields

$$H_z = \frac{\mathrm{H_C}}{4\pi}\sum_{i=1}^{16} S_i\left(H_i^{\mathrm{real}} + H_i^{\mathrm{img}}\right) \tag{14}$$

where

$$H_i^{\mathrm{real}} = \arctan\left(\frac{\left(\frac{\mathrm{T}}{2} + \mathrm{a}_{zi}z\right)\left(\frac{\frac{\mathrm{L}}{2}+\mathrm{a}_{xi}x}{\left|\frac{\mathrm{W}}{2}+\mathrm{a}_{yi}y\right|}\right)^{\mathrm{a}_{ei}}}{R_i}\right) \tag{15}$$

and

$$H_i^{\mathrm{img}} = \arctan\left(\frac{\left(\frac{\mathrm{T}}{2} + \mathrm{a}_{zi}(z+T+\sigma)\right)\left(\frac{\frac{\mathrm{L}}{2}+\mathrm{a}_{xi}x}{\left|\frac{\mathrm{W}}{2}+\mathrm{a}_{yi}y\right|}\right)^{\mathrm{a}_{ei}}}{R_i'}\right) \tag{16}$$

where

$$R_i' = R_i'(x,y,z) = R_i(x,y,z+T+\sigma) \tag{17}$$

The normalized contribution of the three components to the magnetic field are plotted in Fig. 4. One can clearly see the similarities by comparing the x-component and z-component in Fig. 2 to the z-component and x-component in Fig. 4.

3 Head sensitivity

The sensitivity of the read head is defined in a similar way in Yuan and Bertram (1994) as shown in Fig. 5. The shields are assumed to have infinite width and the read element has a finite width w and thickness t. The gap between the read element and the shield is defined as g. The sensitivity function is unique to the head design. In simulations in this paper a sensitivity as indicated in Fig. 5 is assumed. The TMR element reads 100% of the signal and the sensitivity decreases towards the edges of the shield. At the shield, no signal is detected by the read element. Different sensitivity functions are conceivable, such as a Gaussian shaped read sensitivity function (Wachenschwanz et al. 2005).

The read back signal is approximated by the convolution of media magnetization and read element sensitivity function. Using superposition and the analytic model for one single bit allows the computation of the x–y distribution of the read back signal for different flying heights and for arbitrary bit pattern.

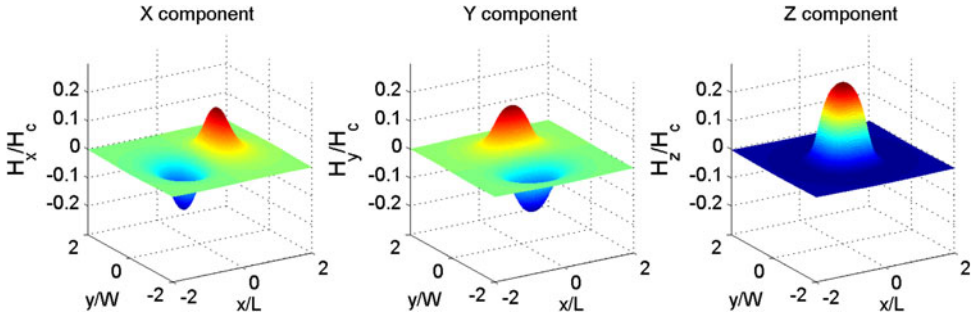

Fig. 4 Normalized magnetic field components for perpendicular magnetic recording measured at HMS = 10 for W = 50, L = 50, T = 20 nm

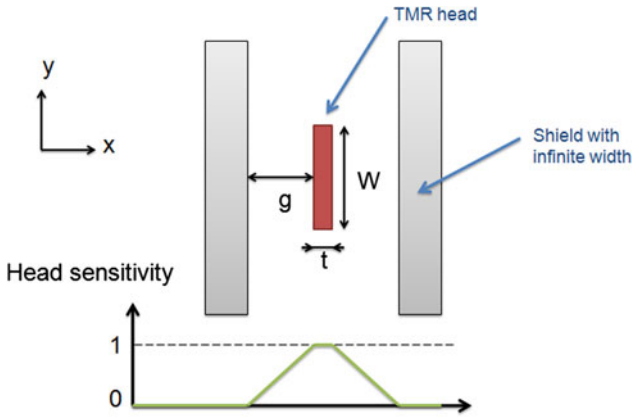

Fig. 5 Assumed TMR head sensitivity function

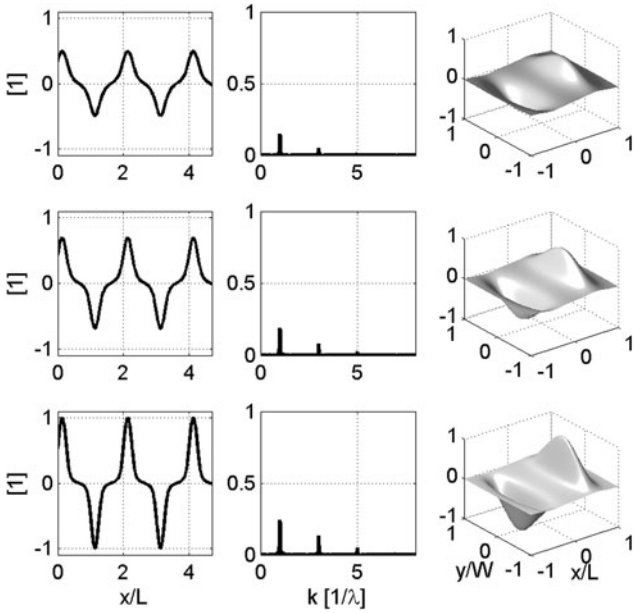

Fig. 6 Normalized LMR read back signal for a head-medium-spacing of 18, 10 and 2 nm. *First column* time/spacial domain, *second column* frequency domain, *third column* read back signal of 1 single bit (normalized by bit length and bit width)

4 Simulation example

As a simulation example, three different head-medium spacings are computed for longitudinal and PMR. Figure 7 shows the computed read back signal for the following assumed parameters: The bit dimensions were defined as $L = 170\,\text{nm}$, $W = 80\,\text{nm}$, $T = 20\,\text{nm}$, $\sigma = 0\,\text{nm}$ and reader parameter were assumed as $w = 60\,\text{nm}$, $g = 30\,\text{nm}$, $t = 10\,\text{nm}$. Figure 6 shows the simulated read back signal based on the above parameters for a "16T"-type pattern that is used in the experimental section in Boettcher et al. (2011). The 16T pattern consists of 8 "up"-magnetized bits followed by 8 "down"-magnetized bits. Three different

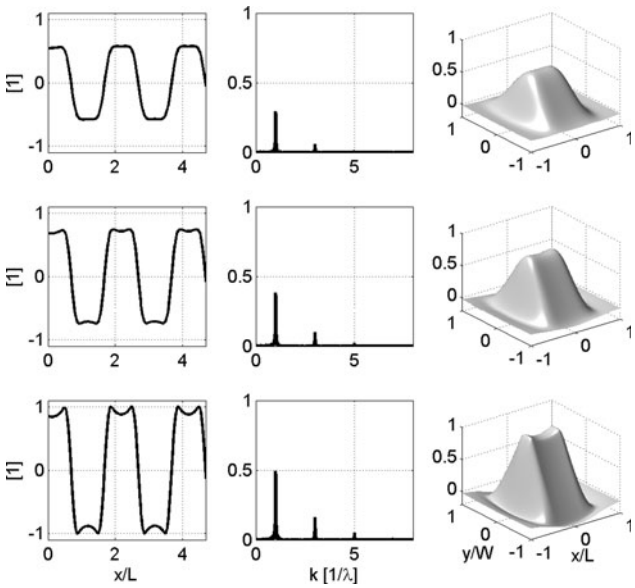

Fig. 7 Normalized PMR read back signal for a head-medium-spacing of 18, 10 and 2 nm. *First column* time/spacial domain, *second column* frequency domain, *third column* read back signal of 1 single bit (normalized by bit length and bit width)

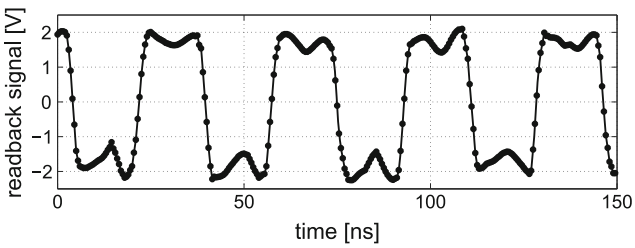

Fig. 8 Raw read back signal of a 16T pattern at approximately 2 nm head-medium-spacing measured on Microphysics spinstand at a write frequency of 450 MHz sampled at 2 GHz

head-medium spacings are shown in Fig. 6: 18, 10 and 2 nm. The left column shows the time domain signal (normalized by the maximum signal at 2 nm HMS) at track center (y = 0); the second column shows the corresponding single sided amplitude of the frequency spectrum and the third column shows the read back signal distribution for one single bit in down-track (x) and off-track (y) direction. In a similar fashion, the read back signal for PMR is shown in Fig. 7. Here, the same bit pattern and bit and head parameters were used and a typical shape for a PMR signal can be observed.

For further verification, the "16T"-type pattern was written at 450 MHz onto a disk using a commercially available spinstand (Microphysics Inc.). The raw read back signal is shown in Fig. 8. We observe the typical U-shape of perpendicular recording signals when written at relatively low linear densities. Furthermore, a good qualitative agreement between Figs. 8 and 7 (bottom left) can be

observed. A quantitative comparison could not be performed since exact media and read element parameters are unknown.

5 Conclusions

The significance of the mathematical model derived in this paper is due to its simplicity. In particular, the magnetic field is computed directly instead of using the transition (derivative) of the magnetization in the read back signal. This allows a very fast simulation, without compromising accuracy. The model is applicable to continuous and BPM. The media magnetization model is separated from the reader sensitivity function. The simulated (perpendicular) read signal is in qualitative agreement with experimentally obtained read back signals.

Acknowledgments We would like to acknowledge Dr. Neil Bertram and Dr. Gordon Hughes for valuable discussions related to the read back signal modeling. Furthermore, we would like to express our gratitude to the anonymous reviewers for their comments that helped improving the manuscript.

References

Bertram N (1994) Theory of magnetic recording. Cambridge University Press, Cambridge, p 40

Boettcher U, Lacey CA, Li H, Amemiya K, de Callafon RA, Talke FE (2011) Servo signal processing for flying height control in hard disk drives. Microsyst Technol. doi:10.1007/s00542-010-1193-7

Chai KS, Liu ZJ, Li JT, Long HH (2006) 3D analysis of medium field with consideration of perpendicular head-medium combinations. In: Asia-Pacific magnetic recording conference, 29 Nov 2006 to 1 Dec 2006, pp 1–2

Hughes GF (1999) Read channels for patterned media. IEEE Trans Magn 35(5):2310–2312

Khizroev S, Litvinov D (2004) Perpendicular magnetic recording. Kluwer, Dordrecht

Mallinson JC, Bertram HN (1984) On the characteristics of pole-keeper head fields. IEEE Trans Magn MAG-20-5, pp 721–723

Radhakrishnan R, Erden MF, He C, Vasic B (2007) Transition response characteristics of heat-assisted magnetic recording and their performance with MTR codes. IEEE Trans Magn 43(6): 2298–2300

Richter HJ (1999) Recent advances in the recording physics of thin-flm media. J Phys D: Appl Phys 32(21):R147–R168

Roscamp TA, Boerner ED, Parker GJ (2002) Three-dimensional modeling of perpendicular reading with a soft underlayer. J Appl Phys 91:8366

Shute HA, Wilton DT, McKirdy DMcA, Jermey PM, Mallinson JC (2006) Analytic three-dimensional response function of a double-shielded magnetoresistive or giant magnetoresistive perpendicular head. IEEE Trans Magn 42(5):1611–1619

Smith N (1993) Reciprocity principles for magnetoresistive heads. IEEE Trans Magn 29(5):2279–2285

Spaldin NA (2003) Magnetic materials: fundamentals and device applications. Cambridge University Press, p 8

Suzuki Y, Nishida Y (2001) Calculation method of GMR head response for double layered perpendicular medium. IEEE Trans Magn 37(4):1337–1339

Suzuki Y, Nishida Y (2003) Exact calculation method for medium field from a perpendicular medium. IEEE Trans Magn 39(5):2633–2635

Suzuki Y, Aoi H, Muraoka H, Nakamura Y (2006) Fast calculation of read field from perpendicular recording medium using head characteristic matrix. In: IEEE international magnetics conference, 2006 (INTERMAG 2006), p 798

Takahashi S, Yamakawa K, Ouchi K (2003) Design of multisurface single pole head for high-density recording. J Appl Phys 93(10):6546–6548

Valcu B, Bertram HN (2002) 3-D analysis of the playback signal in perpendicular recording for an off-centered GMR element. IEEE Trans Magn 38(5):2081–2083

Wachenschwanz D, Wen J, Roddick E, Homola A, Dorsey P, Harper B, Treves D, Bajorek C (2005) Design of a manufacturable discrete track recording medium. IEEE Trans Magn 41(2): 670–675

Wilton DT, McKirdy DMcA, Shute HA, Miles JJ, Mapps DJ (2004) Approximate three-dimensional head fields for perpendicular magnetic recording. IEEE Trans Magn 40(1):148–156

Wood RW, Wilton DT (2008) Readback responses in three dimensions for multilayered recording media configurations. IEEE Trans Magn 44(7):1874–1890

Yuan SW, Bertram HN (1994) Off-track spacing loss of shielded MR heads. IEEE Trans Magn 30(3):1267–1273

Yuan SW, Bertram HN (1996) Erratum: Correction to “Off-track spacing loss of shielded MR heads”. IEEE Trans Magn 32(4):3334